JVI Accepts, published online ahead of print on 27 April 2011
J. Virol. doi:10.1128/JVI.00302-11
Copyright © 2011, American Society for Microbiology and/or the Listed Authors/Institutions. All Rights Reserved.

JVI Accepts published online ahead of print

Revised JVI00302-11 version 4

Ambivalent role of the innate immune response in rabies virus pathogenesis [$]

Running title: Role of the innate immune response in rabies

Damien Chopy[*, ţ], Julien Pothlichet[ţ, §ll], Mireille Lafage[*, ţ], Françoise Mégret[*, ţ], Laurence Fiette[¶], Mustapha Si-Tahar[ţ, §] and Monique Lafon[*, ţ]

*) Institut Pasteur, Unité de Neuroimmunologie Virale, Département de Virologie F-75015 Paris, France

ţ) CNRS, URA3015, F-75015 Paris, France

ŧ) Institut Pasteur, Unité de Défense Innée et Inflammation, Département d'Infection et d'Epidémiologie, F-75015 Paris, France

§) INSERM, U874, F-75015 Paris, France

¶) Institut Pasteur, Unité d'Histopathologie Humaine et Modèles Animaux, F-75015 Paris, France

ll: Present address**:** McGill University, Silvia Vidal's Laboratory, Department of Human Genetics, H3G 0B1, Montréal, Québec, Canada

$ This work was supported by internal grants of Institut Pasteur including PTR 186. Damien Chopy is recipient of a fellowship from French Ministère de l'Enseignement Supérieur et de la Recherche.

Corresponding author: Monique Lafon, monique.lafon@pasteur.fr, tel 33 1 45 68 87 52, fax 33 1 40 61 33 12

Abbreviations used in this article: LGP2, Laboratory of Genetics and Physiology-2; NS, nervous system; RABV, rabies virus; IFN, interferon; RIG-I, retinoic acid-inducible gene-I; SeV, Sendai virus; TG, transgenic; WT, wild type.

JVI Accepts published online ahead of print

ABSTRACT

The neurotropic rabies virus (RABV) has developed several evasive strategies including immunoevasion to successfully infect the nervous system (NS) and trigger a fatal encephalomyelitis. Here, we show that LGP2 expression, a protein known either as a positive or negative regulator of the RIG-I mediated-innate immune response, is restricted in the NS. We use a new transgenic mouse model (LGP2 TG) over-expressing LGP2 to impair RABV innate immune response and thus reveals the role of the RIG-I-mediated innate immune response in RABV pathogenesis. After infection, LGP2 TG exhibit reduced expression of inflammatory/chemoattractive molecules, IFN-β, and IFN-stimulated genes in their NS compared to WT, demonstrating the inhibitory function of LGP2 on RABV innate immune response. Surprisingly, LGP2 TG showed a better viral clearance in the brain and lower morbidity compared to WT, indicating that paradoxically the host innate immune response favors RABV neuroinvasiveness and morbidity. LGP2 TG mice exhibited similar neutralizing antibodies and microglia activation as WT, but a reduction of infiltrating $CD4^+$ T cell and a lower disappearance of infiltrating $CD8^+$ T cells. This occurs concomitantly to a reduced neural expression of the IFN-inducible B7-H1, an immunoevasive protein involved in the elimination of infiltrated $CD8^+$ T cells. Our study shows that host innate immune response favors the infiltration of T cells and, at the same time promotes the $CD8^+$T cells elimination. Thus, RABV exploits, in a certain extent, the innate immune response to develop its immune-evasive strategy.

JVI Accepts published online ahead of print

INTRODUCTION

Rabies virus (RABV) is a RNA-negative strand virus that infects mainly neurons and exploits the nervous system (NS) network, to insure its progression from the site of entry (bite site) up to the site of exit, the salivary glands. RABV virulence relies on several factors such as its capacity to avoid premature death of infected neurons and on its property to escape the immune response. Different mechanisms have been proposed to explain the inefficiency of the immune response against RABV infection (24). RABV infection induces an immune-suppression (6, 53) limits T cells infiltration into the NS (44) and keeps the blood brain barrier tightly closed (37, 45). It also promotes the destruction of migratory $CD8^+$ T cells in the NS through the up-regulation of immune-evasive proteins such as B7-H1 (1, 27, 28). B7-H1 (also known as PD-1 ligand and CD274) is interferon inducible and usually expressed by immune cells. It contributes to dampen proliferation, cytokine production and cytolytic activity (20, 28, 48).

During its migration in the NS, RABV has to deal with the first line of defense against pathogens: the host innate immune response. RABV infection activates the innate immune sensor RIG-I and likely also MDA-5 (15, 22) and triggers a classical type-I-IFN, chemoattractive and inflammatory response in infected cells which could be responsible for setting-up an antiviral environment and triggering an efficient immune response (3, 9, 15, 25, 39, 41, 58). As most viruses, RABV has developed a strategy to counteract the antiviral effect of the type-I IFN response (23, 34, 40, 41, 55, 56). Despite these mechanisms, IFN, chemoattractive and inflammatory responses in the RABV-infected NS are far from being abrogated and RABV successfully infects the NS (28, 58).

Here, we investigate to what extent the innate immune response in the NS is important for RABV immune response efficiency, RABV immune-evasive strategy and pathogenesis. To disturb the innate immune response and so to reveal its role on RABV infection, we

JVI Accepts published online ahead of print

infected a new mouse transgenic model that over-expresses LGP2 (LGP2 TG) with a RABV neuro-virulent strain. LGP2 is described either as a negative or positive regulator of RIG-I-like-receptor-mediated immune response (38, 42, 47). Several reports described LGP2 as a negative regulator of the RIG-I signaling during RNA-negative strand viruses infection such as Sendai virus (SeV) or vesicular stomatitis virus (VSV) (38, 42). Three mechanisms have been proposed to explain the inhibitory mechanism of LGP2 on RIG-I pathways: (i) LGP2 binds to viral dsRNA and prevents RIG-I recognition; (ii) LGP2 binds to RIG-I through a regulatory domain and inhibits RIG-I activation and interaction with IPS-1; and (iii) LGP2 competes with IKK epsilon for binding and activating IPS-1 (2, 31).

After demonstrating the negative function of LGP2 on the innate immune response during RABV infection both *in vitro* and in the NS, we showed that LGP2 expression is restricted in neuronal cells. The impairment of the innate immune response in the NS of transgenic mice makes LGP2 TG mice a proper model to study the contribution of the RIG-I mediated innate immune response on RABV pathogenesis. We compared WT and LGP2 TG mice morbidity and mortality, T cells infiltration, drop of migratory $CD8^+$ T cells and B7-H1 expression in the NS (T cell destruction and B7-H1 overexpression being two features of RABV immunoevasive strategy). We showed that the impairment of the innate immune response leads to a lower morbidity but has no effect on mortality during RABV infection. The innate immune response impairment slows down T cell infiltration, prevents RABV immunoevasive strategy and favors RABV elimination from the brain. Thus, RABV may exploit the host innate immune response to successfully invade the NS of the infected host.

JVI Accepts published online ahead of print

MATERIAL AND METHODS

Cells and virus

Mouse NIH3T3 fibroblasts and dorsal root ganglia, as well as human neuroblastoma cells SKNSH (ATCC HTB11), embryonic kidney cells (Hek293A) (QBiogene), and post-mitotic neurons (NT2N) were prepared and grown as previously described (8, 29, 39). The laboratory RABV strain CVS (CVS-NIV), a highly pathogenic strain causing fatal encephalomyelitis in mice after intramuscular injection (7), and Sendai virus (SeV) were propagated as previously described (50, 52). Cells were infected at a multiplicity of infection of 3 and cultivated at 37°C, in 5% CO_2.

Mice

Transgenic mice overexpressing human *LGP2* (LGP2 TG) were generated using C57BL/6 embryonic cells stably transduced at the one-cell stage with a lentiviral vector encoding for *LGP2* (DHX58 NM_024119) under control of the CMV early enhancer/chicken β-actin (CAG) promoter. Homozygous LGP2 TG mice were born at the Mendelian ratio. They developed, bred normally and have no obvious behavioral changes. Histology analysis performed on two male and two female 15 weeks old LGP2 TG mice revealed no lesion or alteration when considering seventeen distinct organs or tissues (including brain, cerebellum, spinal cord, heart, lung, liver, spleen, thymus, mesenteric lymph node, inguinal lymph node, superficial cervical lymph node, stomach, small intestine, kidney, caecum, colon, testis and ovary; not illustrated). Female C57BL/6 mice (Janvier, France), or LGP2 TG mice, six to eight weeks old were intramuscularly inoculated in both hind legs with 1×10^7 infectious particles of RABV. Disease progression was evaluated by scoring clinical signs and mortality as follows: 0 = normal mice, 1 = ruffled fur, 2 = one paralyzed hind leg, 3 = two paralyzed hind legs and hunched back, 4 = tetraplegia (defined as the total loss of mobility), and 5 =

JVI Accepts published online ahead of print

death. Data were presented as a cumulative clinical score (the individual clinical score for each mouse was added) and as a mortality curve. In other experiments, groups of mice (at least n = 3) were deeply anesthetized and intra cardiacally perfused with saline phosphate buffer (SPB) Mg^{2}+ Ca^{2+}. Organs were collected separately and stored at –80°C before being processed for RNA or protein extraction. For immunohistochemistry, mice were perfused with 4% paraformaldehyde in SPB.

Ethical statement

Animal housing and experimental protocols followed guidelines approved by the French Ministry of Agriculture and Institut Pasteur Ethical committee. The Institut Pasteur is a member of Le Comité 1 Régional d'Ethique pour l'Expérimentation Animale (CREEA) de l'Ile de France.

Antibodies and reagents

Antibodies (Ab) were acquired as follows: rabbit polyclonal anti-LGP2 Ab from Proteintech Group, Ca, USA Inc; mouse polyclonal anti-tubulin from Oncogene Research, USA Products; mouse monoclonal Ab, mAb, (clone Alme-1) from Alexis Biochemicals or rabbit Ab from ProSci Inc. (USA) for detection of RIG-I protein; FITC-conjugated rabbit anti-RABV nucleocapsid Ab from Bio-Rad (Marnes-La-Coquette, France) and anti-RABV N protein mAb (PVA-3) was prepared in the laboratory (32); βIII-tubulin was stained with mouse mAb (clone 5G8) from Promega (France); B7-H1 was detected with the rat mAb (clone MIH5) from eBioscience and the rabbit Ab from Santa Cruz, Inc. (Santa Cruz, CA, USA) for immunofluorescence and western blotting, respectively; the anti-mouse IT-Box-m260 kit from Immuno Tools (GmbH, Friesoythe, Germany) was used to phenotype splenocytes and mononuclear cells infiltrating the NS; Glial fibrillary acidic protein, GFAP, specific Ab (Z

JVI Accepts published online ahead of print

0334) was from DAKO (Trappes, France); peroxidase polymer-labeled anti-rabbit secondary Ab (Histofine®) was from Simple Stain Mouse MAX PO kit (Nicheidi Corporation, Tokyo, Japan); and recombinant human IFN-β (Betaferon) was obtained from Schering, Berlin, Germany.

RNA extraction, RT, and qRT-PCR

Total RNAs were extracted with the QIAGEN reagents: QIAzol, the RNeasy kit (for cells) or the Lipid Tissue Midi kit (for brain, entire spinal cord, or equivalent weight of other tissues). RNA quantity and quality were monitored using spectrophotometry (NanoDrop, Labteck France). RT-PCR was performed using a PX2 Thermal Cycler with 30 cycles of amplification and 18S RNA as a reference (housekeeping gene). cDNA synthesis was performed from 1 µg RNA using SuperScript II Reverse transcriptase (Invitrogen). Real-time PCR (qRT-PCR) was performed in duplicate using the ABI PRISM 7500 Fast Sequence Detector system with Power SYBR Green PCR Master Mix (Applied Biosystems) or Go Taq Master Mix (Promega). After normalization to 18S RNA, the relative abundance of mRNA was obtained by calculation of the difference in threshold cycles of the test and control samples (wild type = mock for tissue or non-infected cells, value set to 1), commonly known as the ΔΔCT method. RABV RNA quantification was normalized to 18S and a standard control. Sequences or references of primers used for RT-PCR are listed in (39) or were purchased from QIAGEN.

LGP2 overexpression and IFN-stimulated gene 56 (ISG56) luciferase reporter assay

Cells were transfected with an expression plasmid encoding LGP2 (DHX58 NM_024119) under the control of a CAG promoter, using the Amaxa cell line Nucleofector kit V (Lonza). The ISG56 luciferase reporter assay was constructed and performed as previously described (5). At 12 h post-transfection, cells were infected for 24 h with RABV. Luminescence and

JVI Accepts published online ahead of print

absorbance in cell lysates were measured to evaluate luciferase and β-galactosidase expression, respectively. Luminescence levels were normalized to absorbance level for each sample, and luminescence for RABV-infected samples was expressed relative to the non-infected samples.

Western blot, histo/cyto-immunostaining and measure of neutralizing antibodies

Western blot was performed and visualized as previously described (35). For immunohistochemistry, transverse brain sections were embedded in paraffin according to routine protocols, and cut to 5-µm slices. The astrocytes were labeled with primary GFAP Ab (1/300) and using the Histofine Simple Stain Mouse MaxPO® kit. Hematoxilin was used as a counterstaining. Positive cells were manually counted at 5–6 fields per mouse (magnification x100), and means were compared between similar brain sections from WT and LGP2 TG mice. RABV- and mock-infected cells were immunostained and analyzed as previously described (35). The rapid fluorescent focus inhibition test was used to assay serum samples as previously described (49).

Inflammatory bioarrays

Bioarrays were performed with 100 µg of brain lysates (90µg/sample) using the Mouse Inflammation Ab Array G series 1 kit from RayBiotech, Inc. GA, USA. Arrays were read on an AxioVision scanner and analyzed using Axon GenePix software. The fluorescence intensity for each spot was normalized to a positive internal control on the array to allow for array comparison. The fluorescence intensity for the WT mock-infected brain was defined as a standard arbitrary value of 100.

JVI Accepts published online ahead of print

Flow cytometry

NS mononuclear cells were collected from homogenates of brain and spinal cord samples onto Percoll™ gradients as described (19). Phenotype of splenocytes and mononuclear cells infiltrating the NS was performed with appropriate pairs of Ab and assessed by flow cytometry. Data analysis was performed with Cell Quest Pro Software.

Statistical analysis

For comparison of groups, Student's t tests were performed using GraphPad Prism version 5.00 for Windows. For the animal experiments, collected data were plotted as Kaplan–Meier survival curves.

JVI Accepts published online ahead of print

RESULTS

LGP2 inhibits the in vitro RABV-mediated type I IFN response

To test LGP2 effect on RABV-mediated IFN response *in vitro,* we studied the induction of Interferon Stimulated Gene-56 (ISG56), one of the most activated genes during RABV infection (39), using an ISG56-dependent luciferase reporter assay in human Hek cells co-transfected with an expression vector encoding human *LGP2* or a mock plasmid and infected with RABV (Fig. 1A). The effect of LGP2 on the transcription of *IFN-β* and the IFN-inducible gene *2'5'oligoadenylate synthetase* 1 (*OAS1*) was also measured by RT-qPCR in LGP2- or mock-transfected cells (Fig. 1B). After a 24-h RABV infection, when LGP2 protein was expressed (Fig. 1A), luminescence activity was two thirds lower in LGP2 overexpressing cells compared to mock-transfected Hek cells (Fig. 1B), and transcription of *IFN-β* and *OAS1* was reduced (Fig. 1B). The lesser induction of *IFN-β* and *OAS1* transcription was not the result of reduced RABV infection in LGP2-transfected cells because RABV infection in LGP2 and mock-transfected Hek cells did not differ (Fig. 1C). Similar results were obtained when mouse NIH3T3 fibroblasts were transfected with *LGP2* (Fig. 1D). These data demonstrated that LGP2 functions as an inhibitor of RABV-triggered IFN-*β* response *in vitro* in both human and mouse cells, suggesting cross reactivity of LGP2 in these two mammalian species.

LGP2 protein expression is restricted in WT mouse brain and neuronal cells even after infection

Because RABV infects the NS, we investigated whether LGP2 is expressed and/or inducible in the NS of the mouse, the animal model of experimental rabies. To characterize *in vivo* the LGP2 expression, we compared LGP2 mRNA and protein expression in the heart, brain, and kidneys from uninfected C57BL/6 mice by qRT-PCR and western blotting (Fig.

JVI Accepts published online ahead of print

2A). Of interest, LGP2 protein expression was barely detectable in brain tissue although mRNAs were present. After an intramuscular injection of RABV, 7 mice were sacrificed at different times post infection (pi) to test LGP2 induction. RABV transcripts and endogenous mLGP2 mRNAs were measured in brain extracts by qRT-PCR (Fig. 2B). We noticed an increase in LGP2 transcripts that paralleled RABV brain invasion. Nevertheless, LGP2 protein expression in the infected brains remained low or barely detectable by western blotting, whereas RIG-I protein was easily detected in the same samples. These results indicated that the brain is almost devoid of LGP2 protein, even after RABV infection.

The low expression of LGP2 in the infected brain might correspond to infiltrated cells or to resident neural cells such as astrocytes (18) or neurons. Because RABV targets mainly neurons, where RABV triggers a RIG-I-mediated innate immune response (22, 39), we further analyzed LGP2 expression in neuronal cells (human post-mitotic neurons, NT2N, and human neuroblastoma, SKNSH). RT-PCR in NT2N cells (Fig. 2C, left panel) and RT-qPCR in SKNSH cells (middle panel) revealed increased *LGP2* transcription in a range similar to that of *RIG-I* transcription. Nevertheless, and in contrast to the results with the RIG-I protein which could be detected in the absence of infection and after infection, LGP2 protein could not be detected under any condition (Fig. 2C, right).

This absence of LGP2 protein was also observed in SKNSH cells after its induction by either a 24-h SeV infection or a 7-h IFN-β treatment (20–1000 UI/ml) (Fig. 2D), two conditions that result in LGP2 transcription up-regulation (26). This indicates that restriction of LGP2 protein expression in neuronal cells was not specific to RABV infection. Further, LGP2 protein expression was observed in cells of non-neuronal origin, such as Hek kidney embryonic cells, after SeV infection or an IFN-β treatment, supporting a neuron-specific restriction of LGP2 expression (Fig. 2E). When proteasome activity was inhibited by MG132 treatment, LGP2 protein could be detected in both non-infected and RABV-infected SKNSH,

JVI Accepts published online ahead of print

suggesting that LGP2 restriction in neuronal cells relies on protein degradation (Fig. 2F). These observations indicated that LGP2 protein expression is naturally restricted in brain and in neuronal cells in particular by cell-specific proteasomal degradation.

LGP2 protein is expressed in the NS of transgenic LGP2 mice

Despite the natural degradation of LGP2 in mouse brain, we investigated whether it was possible to force LGP2 expression in the NS by generating a new transgenic mouse model that overexpresses *LGP2* cDNA downstream from the ubiquitous CAG promoter (LGP2 TG mice). Endogenous and transgenic LGP2 expression was measured and compared by qRT-PCR and western blotting in different organs of wild type (WT) and LGP2 TG mice (Fig. 2G). In LGP2 TG mice, LGP2 expression was observed in all organs tested. However, and despite similar high levels of *LGP2* mRNA in heart and brain (Fig. 2G left), the brain remained the organ with the lowest level of LGP2 protein (Fig. 2G, middle) reflecting the pattern of LGP2 expression already observed in WT mice organs (Fig. 2A). Nevertheless, LGP2 was present in the mouse brain, making the LGP2 TG mouse a relevant model for studying the role of RIG-I mediated innate immune response in RABV immune response and pathogenesis.

LGP2 overexpression drastically impairs the innate immune response in the NS during RABV infection

Histology analysis performed on brain of non-infected LGP2 TG mice showed no activation of glial cells or enhanced brain immune-surveillance (Fig. 3). To test LGP2 function in the innate immune response triggered in the NS during RABV infection, WT and LGP2 TG mice were intramuscularly injected in each hind limb with a dose of an encephalitic

JVI Accepts published online ahead of print

RABV strain expected to kill 80% of the mice. Brain and spinal cords were sampled 8 and 11 days after injection.

The up-regulation of innate immune markers upon RABV infection in the NS of WT mice (transient in spinal cords and sustained in brain, a hallmark of RABV infection) did not occur in the NS of LGP2 TG mice (Fig. 4A). Indeed, after infection, no induction of *IFN-β*, *OAS1*, or *IL-6* was noted compared to mock-infected LGP2 TG mice. This absence of up-regulation of the innate immune response was also observed at the protein level (Fig. 4B). Indeed, in the brains of WT mice, RABV stimulated the expression of 18 markers of inflammation out of the 40 present on the protein array, including chemokines (CCL5, CCL2, CXCL11, and CXCL9), cytokines (IL-6, 12, and 13), and other proteins involved in inflammation (TIMP-1 and 2 and TNFR1). None of these, with the exception of IL-9 and CXCL13, were upregulated by RABV infection in LGP2 TG brains, indicating clearly that the RABV-mediated innate immune response was abrogated in the NS upon LGP2 expression. These data showing that LGP2 overexpression blocks the RABV-induced innate immune response *in vivo* are in agreement with our *in vitro* results (Fig. 1).

LGP2 overexpression reduces RABV morbidity and promotes RABV clearance from the brain

To analyze the effect of the innate immune response impairment on RABV pathogenesis, we compared the progression and outcome of RABV infection in WT and LGP2 TG mice by recording body weight, clinical signs (ruffled fur, hindlimb paralysis, hunchback—a sign of encephalitis, and death) daily up to 20 days pi. As shown in the left panel of Fig. 5A, the weight loss appeared 5 days pi and worsened in both groups as the infection progressed. Nevertheless, the weight loss in LGP2 TG mice was significantly less severe than in WT mice ($p < 0.005$). The cumulative clinical score was significantly decreased in LGP2 TG mice compared to WT mice between days 7 and 12 pi (Fig. 5A, middle panel). Indeed, the mean

JVI Accepts published online ahead of print

delay between the first sign of hunchback and death was significantly greater in LGP2 TG mice compared to WT mice (respectively 2.8 and 1.6 day; $p < 0.05$). However, despite the slower disease progression in LGP2 TG mice, the mortality of LGP2 TG mice did not differ significantly from that of WT mice (75% and 62%, day 20 mortality, respectively; Fig. 5A, right).

RABV neuroinvasiveness was monitored in the spinal cord and brain of RABV-infected WT and LGP2 TG mice by measurement of the amount of N viral gene transcripts (Fig. 5B). Viral transcription was similar between the two groups in the spinal cord at days 8 and 11 pi, whereas it was drastically reduced in the brains of LGP2 TG mice at day 11 pi -(10^7 fold less than in the brains of WT mice)- (Fig. 5B right). In addition, the kinetics of brain invasion indicated that in contrast to WT mice, the LGP2 TG mice had almost cleared the infection from the brain at day 11 pi. Nevertheless, this clearance was not sufficient to protect the mice from a fatal outcome.

In conclusion, LGP2 overexpression, which blocks the innate immune response induced by RABV in the NS, does not modify disease outcome; nevertheless, it favors viral clearance in the LGP2 TG brain and allows significantly reduced signs of disease.

LGP2 overexpression does not modify humoral response and T cells phenotypes in periphery

To study the origin of this viral clearance, we hypothesized that the immune response in the periphery could be more efficient in LGP2 TG than in WT mice. Specific emphasis was given to the humoral response because RABV-specific neutralizing Ab play a crucial role in protection against RABV infection (10). However, the neutralizing Ab reached similar titers in the blood of WT and LGP2 TG mice (Fig. 6A). In addition, the phenotype of immune cells in the spleen of RABV-infected WT and LGP2 TG mice (days 5 and 8 pi) was not significantly different, showing similar CD4/CD8 ratios and a similar proportion of B cells

JVI Accepts published online ahead of print

(Fig. 6B right and left panels respectively). These observations suggest that LGP2 overexpression does not cause major effect in the setting up of the immune response in the periphery.

LGP2 overexpression slows down leukocytes infiltration into the NS and limits destruction of infiltrated CD8$^+$ T cells.

Because activated microglia and infiltrated leukocytes into the inflammatory brain can contribute to viral clearance (46), we compared the activation of microglia and the number of infiltrated leukocytes in the NS of LGP2 TG and WT mice (Fig. 7A).

Percentages of monocytes (CD11b$^+$ cells), microglia (CD11b$^+$ intermediate CD45$^+$) and activated microglia/macrophages (CD11b$^+$ high CD45$^+$) were identical 6 days pi in both groups of mice (Fig. 7A), suggesting that RABV clearance in LGP2 TG mice does not result from higher microglia activation. No difference was seen in B cells infiltration (Fig. 7B). In contrast, the numbers of T cells (TCRα/β$^+$) and CD4$^+$ T cells were lower in LGP2 TG mice brains compared to WT 6 days pi (Fig. 7C and Fig. 7D). This decline in T cells is consistent with the lower inflammatory and chemoattractive response observed in RABV-infected LGP2 NS compared to WT NS (see Fig. 4).

Since T cells-mediated IFN-γ-dependent inflammation has been identified as a factor clearing RABV infection from the NS (19, 21), we analyzed whether IFN-γ expression was different in the NS of LGP2 TG compared to WT. As shown in Fig. 7E, RABV infection up regulates IFN-γ expression in a similar range in both WT and LGP2 TG mice brain (similar data were obtained in spinal cords). These data indicate that higher IFN-γ expression is not responsible for better viral clearance in LGP2 TG mice brain.

Because RABV has evolved immune evasive strategy mainly through the destruction/exhaustion of infiltrated CD8$^+$ T cells in the NS (1, 28), we studied whether the

JVI Accepts published online ahead of print

innate immune response impairment in LGP2 TG mice affects $CD8^+$ T cells elimination and so may explain RABV clearance in transgenic mice brain. For this purpose, we compared the fate of $CD8^+$ T cells in the NS of RABV-infected LGP2 TG and WT mice (Fig. 7F and G). Six days after infection similar amounts of $CD8^+$ T cells were observed in the brain infiltrates of RABV infected LGP2 and WT mice (Fig. 7F, left panel). However, the $CD8^+$ T cells proportion drops from 35% to 12% in WT mice brains between day 5 and day 8 pi whereas this population decreases from 43% to 24% in the infected LGP2 TG brain (Fig. 7F, middle). Thus, the drop of $CD8^+$ T cells among $CD3^+$ cells that occurs between day 5 and day 8 in the RABV infected brains is lower in LGP2 TG mice (-41%) compared to WT (-68%), (Fig. 7F, right panel).

Similarly, when 6 day RABV-infected WT and LGP2 TG mice were sorted according to the severity of clinical signs, (group 1 weight loss < 5% and group 2 weight loss > 5%; Fig. 7G), the expected drop among migratory $CD8^+$ T cells caused by RABV was observed between groups 1 and 2 of WT mice and not between the LGP2 TG groups. These data indicated that LGP2 overexpression is associated with the protection of the migratory $CD8^+$ T cells in the NS.

Altogether, these results indicate that the impairment of the innate immune response in the RABV infected NS of LGP2 TG mice reduces the infiltration of immune migratory cells but keeps constant IFN-γ expression and protects specifically the subpopulation of infiltrated $CD8^+$ T cells.

LGP2 overexpression impairs B7-H1 induction in RABV infected NS and primary neurons.

In RABV-infected WT brain, the drop in migratory $CD8^+$ T cell numbers can result in the up-regulation of B7-H1 protein in the NS (28). Indeed, the expression of the IFN inducible B7-H1 protein contributes to the exhaustion (16) or destruction (13) of $CD8^+$ T cells

JVI Accepts published online ahead of print

that are potentially responsible for RABV clearance (19). In this context, it is expected that a lower level of *B7-H1* expression would be associated with reduced RABV neuroinvasiveness. We therefore compared B7-H1 expression (mRNA and protein) in the NS of RABV infected LGP2 TG and WT mice (Fig. 8A and B). The RABV-mediated up-regulation of *B7-H1* mRNA observed in WT brain at day 8 and 11 pi was significantly reduced in LGP2 TG brains compared to WT mouse brains (10 fold less in LGP2 TG brains) (Fig. 8A, left). Similarly, the RABV-mediated up-regulation of B7-H1 protein observed in WT brains at day 8 or 11 pi was not observed in RABV-infected LGP2 TG brains (Fig. 8B).

We also performed immunocytochemistry of B7-H1 protein expression in primary neuronal cultures prepared from dorsal root ganglia of adult spinal cord of WT and LGP2 TG mice after *in vitro* RABV infection (Fig. 8C). In contrast to neurons obtained from WT mice, in which RABV infection triggered strong B7-H1 protein expression, neurons obtained from LGP2 TG mice, despite an equal level of infection, showed only weak expression of B7-H1 protein upon infection**.**

These data indicated that LGP2 over-expression decreases neuronal B7-H1 expression, a feature consistent with protection of migratory $CD8^+$ T cells and viral clearance from the LGP2 TG mouse brain.

JVI Accepts published online ahead of print

DISCUSSION

In this study, we observed that LGP2 expression is tightly regulated and not ubiquitous, as previously suggested (11, 17, 30). Remarkably, in the absence of infection, neurons and microglia express low levels of LGP2 protein, if they express any, with the exception of *ex vivo* primary astrocytes in cultures (11, 17). In the transgenic LGP2 TG mouse, LGP2 protein expression reached the lowest level in brain when compared with other tissues, despite similar LGP2 transcription. Results with MG132 treatment suggest that LGP2 is actively degraded in neuronal cells and thus cannot exert its inhibitory function in this tissue. Lech and colleagues (30) observed that RIG-I–like helicase distribution varies drastically among tissues suggesting that the knowledge about RIG-I–like helicase distribution is crucial in the design of experiments. This supports the suitable choice of LGP2 overexpression rather than mice lacking LGP2, ($LGP2^{-/-}$ mice), to modulate the innate immune response and address its function in the course of a strictly neurotropic virus infection.

We showed that LGP2 functions as an inhibitor of the innate immune response triggered by RABV infection. Evidence of the inhibitory function of LGP2 on type I IFN response during RABV infection was obtained both *in vivo* and *in vitro* in different cell types. ISG56 expression was reduced in the LGP2-transfected mouse and human fibroblasts (Hek), and LGP2-transfected Hek cells had reduced IFN-β and IFN-related gene expression compared to mock-transfected cells. Moreover, cultures of primary neurons from LGP2 TG mice showed reduced expression of the IFN-regulated protein, B7-H1. These results are in agreement with the inhibitory role of LGP2 previously observed after VSV infection of $LGP2^{-/-}$ mouse embryonic fibroblasts and macrophages (54). In contrast, they were in contradiction with a report describing LGP2 as a positive regulator of the RIG-I pathway in conventional dendritic cells (cDCs) from $LGP2^{-/-}$ mice infected with VSV (47). This finding

JVI Accepts published online ahead of print

may suggest that LGP2 could be a positive regulator specifically in cDCs but not in other cell types (47, 54). In this case, the cell type could determine the inhibitory or positive regulatory function of LGP2. Further studies, such as those comparing the properties of DCs isolated from WT and LGP2 TG mice, will be required to address this point more directly.

Concerning RABV infection, a recent study demonstrates that DC activation after exposure to RABV is dependent on type I IFN receptor signaling rather than on RIG-I signaling (15). The fact that activation of DCs in the periphery relies on a signaling pathway independent of LGP2 regulation may explain why the production of RABV-specific neutralizing antibodies and the phenotype of spleen immune cells did not differ between WT and LGP2 TG mice. These results suggest that the LGP2 TG mice phenotype during RABV infection is mostly driven by the function of LGP2 TG in the NS.

After RABV infection, the LGP2 TG exhibited lower clinical signs. The over-expression of LGP2 and the associated impairment of the innate immune response results in a delay in morbidity (hirsute fur, weight loss, hind limb weakness and paralysis), suggesting that RABV morbidity results of an immunopathology mechanism. RABV infection, on the contrary to other encephalitic virus such as West Nile Virus (4, 51) is characterized by a modest inflammatory response in the NS (27). Nevertheless some cytokines such as IL-6 or IL-12, known to be the main culprits of the immunopathology in other diseases (43), are expressed in the RABV infected NS. The over-expression of LGP2 is accompanied by a reduced expression in IL-6 expression and a down regulation of chemokines CCL9 and CXCL11. In their absence, $CD4^+$ T cells infiltration into the RABV infected NS was reduced. Since migratory T cells have been shown to also participate to RABV morbidity (19, 21, 59), both the limited inflammation and infiltration contribute to the reduction of RABV morbidity in the LGP2 TG mice. Our study confirms the contribution of the innate immunity in the morbidity during neurotropic viral infections (57) and demonstrates that the RIG-I mediated

JVI Accepts published online ahead of print

innate immune response participates to RABV morbidity. Such a finding is not totally unexpected because the contribution of the innate immune response in morbidity has already been observed with other neurotropic viral infections (57). However, it was surprising that LGP2 TG mice, in which innate immune response, including the type I IFN is impaired, did not show higher but lower infection of their brain. The type I IFN has been shown to exert antiviral function in several viral infections. In this line, the lower type I IFN response in the NS of LGP2 TG mice should have resulted in a higher infection of the LGP2 TG mice NS compared to those of WT mice. However, this was not the case since after the peripheral viral injection the spinal cords were equally infected in the two types of mice. This observation, altogether with previous studies investigating the role of IFN in rabies (28, 33, 36) questions the efficiency of IFN to control RABV infection in the NS. In the same line, as several studies having pointed out that infiltrating T cells recruited into the brain by chemokines have a direct antiviral effect on RABV infection (14, 19, 59), it was expected that mice exhibiting reduced T cells infiltration, as LGP2 TG mice do, would be less able to control RABV spread in the NS than WT mice. In striking contrast, LGP2 TG mice and not WT mice eliminate RABV infection from their brain at day 11pi. This discrepancy suggests that factors other than the size of the infiltrates of immune effectors into the brain may contribute to viral clearance. In RABV- infected NS, the infiltrated T cells have been shown to express several markers of activation including IFN-γ (19). The fact that despite a reduction in the pool of migratory T cells, IFN-γ expression was similar in the NS of LGP2 TG and WT mice, suggests that the activation of the infiltrated T cells could be stronger in LGP2 TG mice than in WT mice.

Since, RABV has evolved an immuno-evasive strategy funded on the destruction/exhaustion of infiltrated $CD8^+$ T cells in the NS of infected mice (1, 28), we analyzed whether the drop of $CD8^+$ T cells, a hallmark of RABV infection in the NS of WT mice, has been interrupted in LGP2 TG. We observed that indeed the disappearance of $CD8^+$ T cells was decreased in the

JVI Accepts published online ahead of print

NS of RABV infected LGP2 TG compared to WT. Because we have previously shown that in absence of B7-H1 expression, the pool of migratory $CD8^+$ T cells is preserved and RABV infection in the brain is controlled (28), it was tempting to check whether the expression of this immune-evasive protein expression was decreased in LGP2 TG mice. Indeed, the $CD8^+$ T cells persistence in LGP2 mice is concomitant with reduced expression of the IFN inducible B7-H1 protein. Here we show that neurons were co-stained with B7-H1 in DRG cultures. Tumor cells, dendritic cells, neurons and astrocytes are the cells most commonly expressing B7-H1, but T cells can also express B7-H1 in certain conditions (12, 28, 48). Previous study has shown no evidence that infiltrated $CD3^+$ T cells expressed B7-H1 in the RABV infected brain (28). We cannot completely exclude that some T cells contribute to B7-H1 expression in the NS of infected mice but this contribution should be modest. Thus, we propose that B7-H1 down regulation in neural cells probably rely on a type I IFN dependent mechanism.

These data indicate that innate immune impairment correlates with a decrease of T cells infiltration, B7-H1 induction and a preservation of activated $CD8^+$ T cells in LGP2 TG mice brain. Altogether these mechanisms might explain RABV clearance in the brain seen in LGP2 TG mice.

Despite virus clearance, mortality of LGP2 TG mice was not different from WT, suggesting that the compensatory mechanism resulting of the protection of the $CD8^+$ T cells as discussed above is insufficient to counterbalance the lower T cell infiltration and to avoid death. In a previous study, when B7-$H1^{-/-}$ mice were infected by RABV, mortality was drastically reduced and the severity of RABV pathogenesis was inversely correlated with the number of $CD8^+$ T cells in the NS (28). This apparent discrepancy concerning the role of RABV immuno-evasion on disease outcome may be explained by the lower T cells infiltration in LGP2 TG NS compared to WT mice. This lower T cells infiltration probably

JVI Accepts published online ahead of print

leads to a less efficient RABV elimination in LGP2 TG compared to B7-H1$^{-/-}$ mice. Exact mechanisms causing death in rabies are not well understood, some may be related to neuronal exhaustion and hormonal deregulation resulting in a lethal "stress" (53). Delay in viral clearance such as those observed in LGP2 TG may result in an exposure to RABV-mediated "stress" long enough to cause the host death.

Altogether, our results suggest that RABV circumvents the host IFN response in only a limited extend and that the escaped amount of IFN is sufficient to stimulate B7-H1 expression. Thus, we surmise that the efficiency of RABV immune-evasion relies paradoxically on the protective mechanism triggered by the host to fight the infection. In this line, it is tempting to propose that the absence of LGP2 in the NS could be a factor that also favors completion of the life cycle of this strictly neurotropic virus.

JVI Accepts published online ahead of print

ACKNOWLEDGMENTS

We are grateful to Christophe Préhaud for helpful advice; Eliane Meurs, Stephanie Dabo, and Damien Vitour, Unité Immunité des Hepacivirus, Institut Pasteur, for helpful discussions and supplying reagents; Viviane Balloy, Unité de Défense Innée et Inflammation, headed by Michel Chignard at the Institut Pasteur, for breeding the LGP2 mice; Dominique Come, Unité de Recherche et d'Expertise en Histotechnologie et Pathologie, Institut Pasteur, for skillful help with immunohistochemistry experiments; and Odile Sismeiro from Puces à ADN core facility, Institut Pasteur, for kind help with the AxioVision scanner.

JVI Accepts published online ahead of print

REFERENCES

1. **Baloul, L., S. Camelo, and M. Lafon.** 2004. Up-regulation of Fas ligand (FasL) in the central nervous system: a mechanism of immune evasion by rabies virus. J Neurovirol **10:**372-82.
2. **Bamming, D., and C. M. Horvath.** 2009. Regulation of signal transduction by enzymatically inactive antiviral RNA helicase proteins MDA5, RIG-I, and LGP2. J Biol Chem **284:**9700-12.
3. **Blondel, D., T. Regad, N. Poisson, B. Pavie, F. Harper, P. P. Pandolfi, H. De The, and M. K. Chelbi-Alix.** 2002. Rabies virus P and small P products interact directly with PML and reorganize PML nuclear bodies. Oncogene **21:**7957-70.
4. **Brehin, A.-C., J., Mouries, M.-P., Frenkiel, G., Dadaglio, P., Despres, M., Lafon, and T. Couderc.** 2008. Dynamics of immune cell recruitment during West Nile encephalitis and identification of a new CD19+ B220- BST-2+ leukocyte population. Journal of Immunology **180:**6760-6767.
5. **Breiman, A., N. Grandvaux, R. Lin, C. Ottone, S. Akira, M. Yoneyama, T. Fujita, J. Hiscott, and E. F. Meurs.** 2005. Inhibition of RIG-I-dependent signaling to the interferon pathway during hepatitis C virus expression and restoration of signaling by IKKepsilon. J Virol **79:**3969-78.
6. **Camelo, S., M. Lafage, A. Galelli, and M. Lafon.** 2001. Selective role for the p55 Kd TNF-alpha receptor in immune unresponsiveness induced by an acute viral encephalitis. J Neuroimmunol **113:**95-108.
7. **Camelo, S., M. Lafage, and M. Lafon.** 2000. Absence of the p55 Kd TNF-alpha receptor promotes survival in rabies virus acute encephalitis. J Neurovirol **6:**507-18.
8. **Castellanos, J. E., M. Martinez-Gutierrez, H. Hurtado, R. Kassis, H. Bourhy, O. Acosta, and M. Lafon.** 2005. Studying neurotrophin antiviral effect on rabies-infected dorsal root ganglia cultures. J Neurovirol **11:**403-10.
9. **Chelbi-Alix, M. K., A. Vidy, J. El Bougrini, and D. Blondel.** 2006. Rabies viral mechanisms to escape the IFN system: the viral protein P interferes with IRF-3, Stat1, and PML nuclear bodies. J Interferon Cytokine Res **26:**271-80.
10. **Cox, J. H., B. Dietzschold, and L. G. Schneider.** 1977. Rabies virus glycoprotein. II. Biological and serological characterization. Infect Immun **16:**754-9.
11. **Cui, S., K. Eisenacher, A. Kirchhofer, K. Brzozka, A. Lammens, K. Lammens, T. Fujita, K. K. Conzelmann, A. Krug, and K. P. Hopfner.** 2008. The C-terminal regulatory domain is the RNA 5'-triphosphate sensor of RIG-I. Mol Cell **29:**169-79.
12. **Dong, H., and L. Chen.** 2003. B7-H1 pathway and its role in the evasion of tumor immunity. J Mol Med **81:**281-7.
13. **Dong, H., S. E. Strome, D. R. Salomao, H. Tamura, F. Hirano, D. B. Flies, P. C. Roche, J. Lu, G. Zhu, K. Tamada, V. A. Lennon, E. Celis, and L. Chen.** 2002. Tumor-associated B7-H1 promotes T-cell apoptosis: a potential mechanism of immune evasion. Nat Med **8:**793-800.
14. **Fabis, M. J., T. W. Phares, R. B. Kean, H. Koprowski, and D. C. Hooper.** 2008. Blood-brain barrier changes and cell invasion differ between therapeutic

JVI Accepts published online ahead of print

immune clearance of neurotrophic virus and CNS autoimmunity. Proc Natl Acad Sci U S A **105:**15511-6.

15. **Faul, E. J., C. N. Wanjalla, M. S. Suthar, M. Gale, C. Wirblich, and M. J. Schnell.** 2010. Rabies virus infection induces type I interferon production in an IPS-1 dependent manner while dendritic cell activation relies on IFNAR signaling. PLoS Pathog **6:**e1001016.
16. **Freeman, G. J., A. J. Long, Y. Iwai, K. Bourque, T. Chernova, H. Nishimura, L. J. Fitz, N. Malenkovich, T. Okazaki, M. C. Byrne, H. F. Horton, L. Fouser, L. Carter, V. Ling, M. R. Bowman, B. M. Carreno, M. Collins, C. R. Wood, and T. Honjo.** 2000. Engagement of the PD-1 immunoinhibitory receptor by a novel B7 family member leads to negative regulation of lymphocyte activation. J Exp Med **192:**1027-34.
17. **Furr, S. R., V. S. Chauhan, D. Sterka, Jr., V. Grdzelishvili, and I. Marriott.** 2008. Characterization of retinoic acid-inducible gene-I expression in primary murine glia following exposure to vesicular stomatitis virus. J Neurovirol **14:**503-13.
18. **Furr, S. R., M. Moerdyk-Schauwecker, V. Z. Grdzelishvili, and I. Marriott.** 2010. RIG-I mediates nonsegmented negative-sense RNA virus-induced inflammatory immune responses of primary human astrocytes. Glia **58:**1620-9.
19. **Galelli, A., L. Baloul, and M. Lafon.** 2000. Abortive rabies virus central nervous infection is controlled by T lymphocyte local recruitment and induction of apoptosis. J Neurovirol **6:**359-72.
20. **Greenwald, R. J., G. J. Freeman, and A. H. Sharpe.** 2005. The B7 Family Revisited. Annu Rev Immunol **23:**515-548.
21. **Hooper, D. C., K. Morimoto, M. Bette, E. Weihe, H. Koprowski, and B. Dietzschold.** 1998. Collaboration of antibody and inflammation in clearance of rabies virus from the central nervous system. J Virol **72:**3711-9.
22. **Hornung, V., J. Ellegast, S. Kim, K. Brzozka, A. Jung, H. Kato, H. Poeck, S. Akira, K. K. Conzelmann, M. Schlee, S. Endres, and G. Hartmann.** 2006. 5'-Triphosphate RNA is the ligand for RIG-I. Science **314:**994-7.
23. **Ito, N., G. W. Moseley, D. Blondel, K. Shimizu, C. L. Rowe, Y. Ito, T. Masatani, K. Nakagawa, D. A. Jans, and M. Sugiyama.** 2010. Role of interferon antagonist activity of rabies virus phosphoprotein in viral pathogenicity. J Virol **84:**6699-710.
24. **Johnson, N., A. F. Cunningham, and A. R. Fooks.** 2010. The immune response to rabies virus infection and vaccination. Vaccine **28:**3896-901.
25. **Johnson, N., C. S. McKimmie, K. L. Mansfield, P. R. Wakeley, S. M. Brookes, J. K. Fazakerley, and A. R. Fooks.** 2006. Lyssavirus infection activates interferon gene expression in the brain. J Gen Virol **87:**2663-7.
26. **Komuro, A., and C. M. Horvath.** 2006. RNA- and virus-independent inhibition of antiviral signaling by RNA helicase LGP2. J Virol **80:**12332-42.
27. **Lafon, M.** 2008. Immune evasion, a critical strategy for rabies virus. Dev Biol (Basel) **131:**413-9.
28. **Lafon, M., F. Megret, S. G. Meuth, O. Simon, M. L. Velandia Romero, M. Lafage, L. Chen, L. Alexopoulou, R. A. Flavell, C. Prehaud, and H. Wiendl.** 2008. Detrimental contribution of the immuno-inhibitor b7-h1 to rabies virus encephalitis. J Immunol **180:**7506-15.

JVI Accepts published online ahead of print

29. **Lafon, M., C. Prehaud, F. Megret, M. Lafage, G. Mouillot, M. Roa, P. Moreau, N. Rouas-Freiss, and E. D. Carosella.** 2005. Modulation of HLA-G expression in human neural cells after neurotropic viral infections. J Virol **79:**15226-37.
30. **Lech, M., A. Avila-Ferrufino, V. Skuginna, H. E. Susanti, and H. J. Anders.** 2010. Quantitative expression of RIG-like helicase, NOD-like receptor and inflammasome-related mRNAs in humans and mice. Int Immunol **22:**717-28.
31. **Li, X., C. Lu, M. Stewart, H. Xu, R. K. Strong, T. Igumenova, and P. Li.** 2009. Structural basis of double-stranded RNA recognition by the RIG-I like receptor MDA5. Arch Biochem Biophys **488:**23-33.
32. **Libeau, G., and M. Lafon.** 1984. Production of monoclonal antibodies against the Pasteur (P.V.) strain of rabies virus: problems and results. Dev Biol Stand **57:**213-8.
33. **Lodmell, D. L., D. L. Wiedbrauk, and L. C. Ewalt.** 1989. Interferon induced within the central nervous system during infection is inconsequential as a mechanism responsible for murine resistance to street rabies virus. J Gen Virol **70 (Pt 2):**473-8.
34. **Masatani, T., N. Ito, K. Shimizu, Y. Ito, K. Nakagawa, Y. Sawaki, H. Koyama, and M. Sugiyama.** 2010. Rabies virus nucleoprotein functions to evade activation of the RIG-I-mediated antiviral response. J Virol **84:**4002-12.
35. **Menager, P., P. Roux, F. Megret, J. P. Bourgeois, A. M. Le Sourd, A. Danckaert, M. Lafage, C. Prehaud, and M. Lafon.** 2009. Toll-like receptor 3 (TLR3) plays a major role in the formation of rabies virus Negri Bodies. PLoS Pathog **5:**e1000315.
36. **Mendonca, R. Z., and C. A. Pereira.** 1994. Relationship of interferon synthesis and the resistance of mice infected with street rabies virus. Braz J Med Biol Res **27:**691-5.
37. **Phares, T. W., R. B. Kean, T. Mikheeva, and D. C. Hooper.** 2006. Regional differences in blood-brain barrier permeability changes and inflammation in the apathogenic clearance of virus from the central nervous system. J Immunol **176:**7666-75.
38. **Pippig, D. A., J. C. Hellmuth, S. Cui, A. Kirchhofer, K. Lammens, A. Lammens, A. Schmidt, S. Rothenfusser, and K. P. Hopfner.** 2009. The regulatory domain of the RIG-I family ATPase LGP2 senses double-stranded RNA. Nucleic Acids Res **37:**2014-25.
39. **Prehaud, C., F. Megret, M. Lafage, and M. Lafon.** 2005. Virus infection switches TLR-3-positive human neurons to become strong producers of beta interferon. J Virol **79:**12893-904.
40. **Rieder, M., K. Brzozka, C. K. Pfaller, J. H. Cox, L. Stitz, and K. K. Conzelmann.** 2011. Genetic dissection of interferon-antagonistic functions of rabies virus phosphoprotein: inhibition of interferon regulatory factor 3 activation is important for pathogenicity. J Virol **85:**842-52.
41. **Rieder, M., and K. K. Conzelmann.** 2009. Rhabdovirus evasion of the interferon system. J Interferon Cytokine Res **29:**499-509.
42. **Rothenfusser, S., N. Goutagny, G. DiPerna, M. Gong, B. G. Monks, A. Schoenemeyer, M. Yamamoto, S. Akira, and K. A. Fitzgerald.** 2005. The RNA helicase Lgp2 inhibits TLR-independent sensing of viral replication by retinoic acid-inducible gene-I. J Immunol **175:**5260-8.

JVI Accepts published online ahead of print

43. **Rouse, B. T., and S. Sehrawat.** 2010. Immunity and immunopathology to viruses: what decides the outcome? Nat Rev Immunol **10:**514-26.
44. **Roy, A., and D. C. Hooper.** 2008. Immune evasion by rabies viruses through the maintenance of blood-brain barrier integrity. J Neurovirol **14:**401-11.
45. **Roy, A., and D. C. Hooper.** 2007. Lethal silver-haired bat rabies virus infection can be prevented by opening the blood-brain barrier. J Virol **81:**7993-8.
46. **Roy, A., T. W. Phares, H. Koprowski, and D. C. Hooper.** 2007. Failure to open the blood-brain barrier and deliver immune effectors to central nervous system tissues leads to the lethal outcome of silver-haired bat rabies virus infection. J Virol **81:**1110-8.
47. **Satoh, T., H. Kato, Y. Kumagai, M. Yoneyama, S. Sato, K. Matsushita, T. Tsujimura, T. Fujita, S. Akira, and O. Takeuchi.** 2010. LGP2 is a positive regulator of RIG-I- and MDA5-mediated antiviral responses. Proc Natl Acad Sci U S A **107:**1512-7.
48. **Schreiner, B., M. Mitsdoerffer, B. C. Kieseier, L. Chen, H. P. Hartung, M. Weller, and H. Wiendl.** 2004. Interferon-beta enhances monocyte and dendritic cell expression of B7-H1 (PD-L1), a strong inhibitor of autologous T-cell activation: relevance for the immune modulatory effect in multiple sclerosis. J Neuroimmunol **155:**172-82.
49. **Smith, J. S., P. A. Yager, and G. M. Baer.** 1973. A rapid tissue culture test for determining rabies neutralizing antibody. Monogr Ser World Health Organ**:**354-7.
50. **Strahle, L., J. B. Marq, A. Brini, S. Hausmann, D. Kolakofsky, and D. Garcin.** 2007. Activation of the beta interferon promoter by unnatural Sendai virus infection requires RIG-I and is inhibited by viral C proteins. J Virol **81:**12227-37.
51. **Suthar, M. S., D. Y. Ma, S. Thomas, J. M. Lund, N. Zhang, S. Daffis, A. Y. Rudensky, M. J. Bevan, E. A. Clark, M. K. Kaja, M. S. Diamond, and M. Gale, Jr.** 2010. IPS-1 is essential for the control of West Nile virus infection and immunity. PLoS Pathog **6:**e1000757.
52. **Thoulouze, M. I., M. Lafage, J. A. Montano-Hirose, and M. Lafon.** 1997. Rabies virus infects mouse and human lymphocytes and induces apoptosis. J Virol **71:**7372-80.
53. **Torres-Anjel, M. J., D. Volz, M. J. Torres, M. Turk, and J. G. Tshikuka.** 1988. Failure to thrive, wasting syndrome, and immunodeficiency in rabies: a hypophyseal/hypothalamic/thymic axis effect of rabies virus. Rev Infect Dis **10 Suppl 4:**S710-25.
54. **Venkataraman, T., M. Valdes, R. Elsby, S. Kakuta, G. Caceres, S. Saijo, Y. Iwakura, and G. N. Barber.** 2007. Loss of DExD/H box RNA helicase LGP2 manifests disparate antiviral responses. J Immunol **178:**6444-55.
55. **Vidy, A., M. Chelbi-Alix, and D. Blondel.** 2005. Rabies virus P protein interacts with STAT1 and inhibits interferon signal transduction pathways. J Virol **79:**14411-20.
56. **Vidy, A., J. El Bougrini, M. K. Chelbi-Alix, and D. Blondel.** 2007. The nucleocytoplasmic rabies virus P protein counteracts interferon signaling by inhibiting both nuclear accumulation and DNA binding of STAT1. J Virol **81:**4255-63.
57. **Wang, T., T. Town, L. Alexopoulou, J. F. Anderson, E. Fikrig, and R. A. Flavell.** 2004. Toll-like receptor 3 mediates West Nile virus entry into the brain causing lethal encephalitis. Nat Med **10:**1366-73.

JVI Accepts published online ahead of print

58. **Wang, Z. W., L. Sarmento, Y. Wang, X. Q. Li, V. Dhingra, T. Tseggai, B. Jiang, and Z. F. Fu.** 2005. Attenuated rabies virus activates, while pathogenic rabies virus evades, the host innate immune responses in the central nervous system. J Virol **79:**12554-65.

59. **Zhao, L., H. Toriumi, Y. Kuang, H. Chen, and Z. F. Fu.** 2009. The roles of chemokines in rabies virus infection: overexpression may not always be beneficial. J Virol **83:**11808-18.

JVI Accepts published online ahead of print

FIGURE LEGENDS

Figure 1: LGP2 inhibits the type I IFN response during RABV infection *in vitro*. (A) Hek cells were co-transfected with a plasmid encoding a luciferase reporter under the control of an ISG56 promoter, a β-galactosidase–encoding plasmid (used as transfection efficiency control) together with an empty vector (Mock) or an *LGP2*-encoding vector (LGP2). LGP2 protein overexpression was checked by western blotting, with tubulin used as the internal control. After 24 h, luciferase activity was measured by bioluminescence in RABV-infected cells (n = 4). Data are presented as mean ± SEM (*** $p \leq 0.0005$). (B) Hek cells transfected with *LGP2*-encoding vector (LGP2) or an empty vector (Mock) were infected with RABV. RNAs were extracted 24 h pi and qRT-PCR targeting *IFN-β* and *OAS1* was performed (n = 6). Data are presented as mean ± SEM (* $p \leq 0.05$). (C) After 24 h, RABV infection was monitored in LGP2 (LGP2)- and empty vector (Mock)-transfected cells by qRT-PCR (left panel) and by western blotting against the RABV N protein (right panel). Data are representative of two independent experiments. qRT-PCR results are presented as mean ± SEM. (D) NIH3T3 cells were co-transfected as described in (A). After 24 h, luciferase activity was measured by bioluminescence in non-infected (NI) and RABV-infected cells (n = 4). Data are presented as mean ± SEM (*** $p \leq 0.0005$).

Figure 2: LGP2 protein expression is strongly restricted in mouse brain and human neuronal cells because of its degradation. (A) *LGP2* mRNA (upper graph) and LGP2 protein (lower graph) expression were quantified in the heart, brain, and kidney of WT mice by qRT-PCR and normalized to the *LGP2* mRNA level in the kidney (value taken as 1) or by western blotting normalized to tubulin. qRT-PCR data are presented as mean ± SEM (n = 4). (B) Seven RABV-infected mice were sacrificed at different times after virus injection (the first 4 mice were sacrificed at day 6pi and the last 4 at day 9 pi). Brains were separated into

JVI Accepts published online ahead of print

two parts. One half-brain was used for qRT-PCR, the other for western blotting. RABV *N protein* and endogenous m*LGP2* mRNA were quantified in the brain of RABV-infected WT mice or non-infected (NI) animals by qRT-PCR (high panel). LGP2, RIG-I (used as control protein) and tubulin (used as a gel loading control) protein expression in the brains of sacrificed mice was monitored using western blotting (low panel). Positive control (+) is LGP2 expression in a WT heart lysate. (C) *LGP2* and *RIG-I* expression were measured in human post-mitotic neurons (NT2N) and neuroblastoma SKNSH cells after RABV infection (24 h for NT2N and 7, 15, 24, and 48 h for SKNSH) or not (NI) by RT-PCR (NT2N with 18S as an internal control) and by qRT-PCR (SKNSH) (values normalized with NI as value 1). Proteins were detected by western blotting on SKNSH with a heart lysate as a positive control (+) for LGP2 protein (n = 3). (D) LGP2 expression was measured in SKNSH cells 24 h after SeV infection by western blotting (left panel; SeV N protein expression was used as a control for infection), and 7 h after treatment with increasing doses of IFN-β (20, 100, 200, or 500 IU/ml) by western blotting (central panel; RIG-I expression used as control for IFN-β treatment efficiency) and qRT-PCR (normalized with mock value taken as 1). (E) LGP2 expression was measured by western blotting in non-neuronal cells (Hek) 24 h after SeV infection (left panel) and 7 h treatment with increasing IFN-β doses (right panel). SeV N protein expression was used as a control for infection, RIG-I as a control of IFN-β treatment efficacy and tubulin as control of protein loading. (F) Western blotting showing the effect of MG-132 treatment (10 µM) on LGP2 expression in NI and RABV-infected SKNSH cells. (G) LGP2 expression in the brain of LGP2 TG mice. LGP2 protein and *LGP2* mRNA expression were analyzed by qRT-PCR normalized to LGP2 transgenic mRNA levels in kidney (n = 4) (left panel), data are presented as mean ± SEM, and by western blotting in lysates of heart, liver, brain, lung, thymus, muscle, testis, pancreas, and kidney of LGP2 TG (LGP2) and WT mice (right panels). Tubulin is used as a control of protein loading.

JVI Accepts published online ahead of print

Figure 3: LGP2 overexpression in LGP2 TG mice does not modify basal gliosis and monocytes influx into the brain. (A) Astrogliosis was assayed by immunohistochemistry in non-infected WT and LGP2TG paraffin-embedded brain sections using a GFAP primary Ab. Numbers of $GFAP^+$ cells in WT and LGP2TG in caudal diencephalon were 44.6 ± 4.2 and 51.3 ± 3.1 for WT and LGP2TG mice, respectively (20 fields were counted). (B) Flow cytometry of cells isolated from the NS of WT and LGP2TG mice by Percoll gradient and double-stained with CD11b and CD45 Abs to analyze monocytes infiltration and microglia activation. The $CD11b^+$ cells correspond to infiltrated monocytes (9.7 and 7.5 % in WT and LGP2 TG mice respectively) and the $CD11b^+$ $CD45^+$ intermediate cells are microglia cells (1% in both types of mice). Results are representative of two independent experiments.

Figure 4: LGP2 inhibits RABV-triggered type 1 IFN and inflammatory responses in the infected NS. (A) *IFN-β*, *OAS1*, and *IL-6* transcripts were quantified by qRT-PCR in the spinal cord (upper row) and the brain (lower row) of WT and LGP2 TG mice sacrificed on day 8 and day 11 pi (n = 7–8) and normalized to values obtained in mock-infected tissues (value set to 1). Data are presented as mean ± SEM (* $p \leq 0.05$, ** $p \leq 0.005$, *** $p \leq 0.0005$). (B) Inflammatory bioarray for markers of IFN-mediated and inflammatory responses [IL-12p40p70, CXCL9, TIMP-1, sTNF-R1, CCL5, IL-13, CXCL11, CCL2 and IL-6] were compared in NI and RABV-infected brains of WT and LGP2 TG mice at days 8 and 11 pi (n = 2). (Normalized value = 100 for NI WT mouse brain). The results are representative of two independent experiments.

Figure 5: Forced expression of LGP2 slows down RABV clinical progression and favors RABV clearance off the brain. WT and LGP2 TG mice (n = 8) were injected intramuscularly with a dose of an encephalitic strain of RABV sufficient to kill 80% of

JVI Accepts published online ahead of print

injected mice. (A) Clinical signs of rabies (body weight loss, cumulative clinical scores, and mortality curves) were followed in WT (black) and LGP2 TG mice (grey). Results are representative of at least three independent experiments. (B) RABV neuroinvasiveness was compared in the spinal cords and brains of WT and LGP2 TG mice by qRT-PCR targeting RABV N protein at 8 and 11 d pi (n = 7–8). Data are presented as mean ± SEM (* $p \leq 0.05$).

Figure 6: Innate immune impairment does not modify immune parameters in the periphery. (A) RABV-specific neutralizing Ab titers (expressed in international unit per ml, IU/ml) in the blood were compared by the rapid fluorescent focus inhibition technique in WT and LGP2TG mice sera taken 11 d pi (n = 9, 8, respectively) (B) LGP2TG and WT mice exhibit similar spleen sub-populations**.** Spleen cells of RABV-infected WT and LGP2TG mice (n = 4) were taken at days 5 and 8 pi and stained with paired Abs, CD4 and CD8 or B220 and CD19. Percentage of $CD4^+$ $CD8^+$ and $CD19^+$ $B220^+$ cell populations were analyzed by flow cytometry. Results are presented as the $CD4^+/CD8^+$ ratio and percentage of $B220^+$ $CD19^+$ cells (n=8).

Figure 7: Innate immune impairment does not modify activation of microglia, or IFN-γ mRNA expression, but inhibits T cells infiltration and prevents $CD8^+$ T cells destruction into RABV infected brains.

(A) Microglia activation was analyzed by flow cytometry among cells isolated from the NS of day 6 RABV-infected WT and LGP2TG mice by Percoll gradient and double-stained with CD11b and CD45 Abs. Results are representative of two independent experiments. The numbers of monocytes ($CD11b^+$ cells), microglia/macrophage ($CD11b^+$, intermediate and high $CD45^+$) and activated microglia/macrophages ($CD11b^+$, high $CD45^+$) were compared in the infiltrates of 6 days RABV-infected WT and LGP2 TG mice (n=6). (B) Kinetics of

JVI Accepts published online ahead of print

infiltrated B cells ($B220^+$, $CD19^+$) were compared in NI, day 5 and day 8 RABV-infected WT and LGP2 TG mice (n =6). (C) T cells (TCR α/β^+) infiltration of the NS was compared in the two types of mice, 6 day pi, (n=6). Data are presented as the mean of the total infiltrated cells ± SEM. * $p<0.05$. (D) $CD4^+$ T cells infiltration in day 6 infected NS was compared between WT and LGP2 TG mice (***p<0.005).* (E) *IFN-γ* transcripts were quantified by qRT-PCR in the brain of WT and LGP2 TG mice sacrificed day 8 and day 11 pi (n = 7–8) and normalized to values obtained in non-infected (NI) tissues (value set to 1). Data are presented as mean ± SEM. (F) Comparison of $CD8^+$ T cells infiltration in the NS of RABV infected WT and LGP2 TG mice. Left panel: $CD8^+$ T cells infiltration was compared in the infected NS of WT and LGP2 TG mice 6 day pi. Middle panel: Flow cytometry diagrams of CD8 and CD3 double-stained cells isolated from the NS of WT and LGP2 TG mice 5 and 8 d pi. Numbers on the quadrant correspond to the percentage of $CD8^+$ T cells among $CD3^+$ T cells ($CD8^+/CD3^+$). Right panel: Drop in $CD8^+$ T cells between day 5 and day 8 were compared in WT and LGP2 TG mice, (n=6) (**p<0.05, **p<0.005).* (G) Flow cytometry analysis of cells isolated from the NS of WT and LGP2 TG mice and double-stained with CD8 and TCR α/β or CD8 and CD3 pair Abs. Percentages of $CD8^+$T cells among TCR α/β^+ cells were compared in the NS of two groups (1 and 2) of WT and LGP2 mice at day 6 pi. Groups 1 and 2 were determined according to the severity of clinical signs: group 1, weight loss <5% initial body weight, mild clinical signs; group 2, weight loss >5% of initial body weight, severe clinical signs, (n = 4 in each group). Data are represented as the mean of the percentage $CD8^+$T cells among TCR alpha beta $^+$ cells ± SEM (** $p \leq 0.005$).

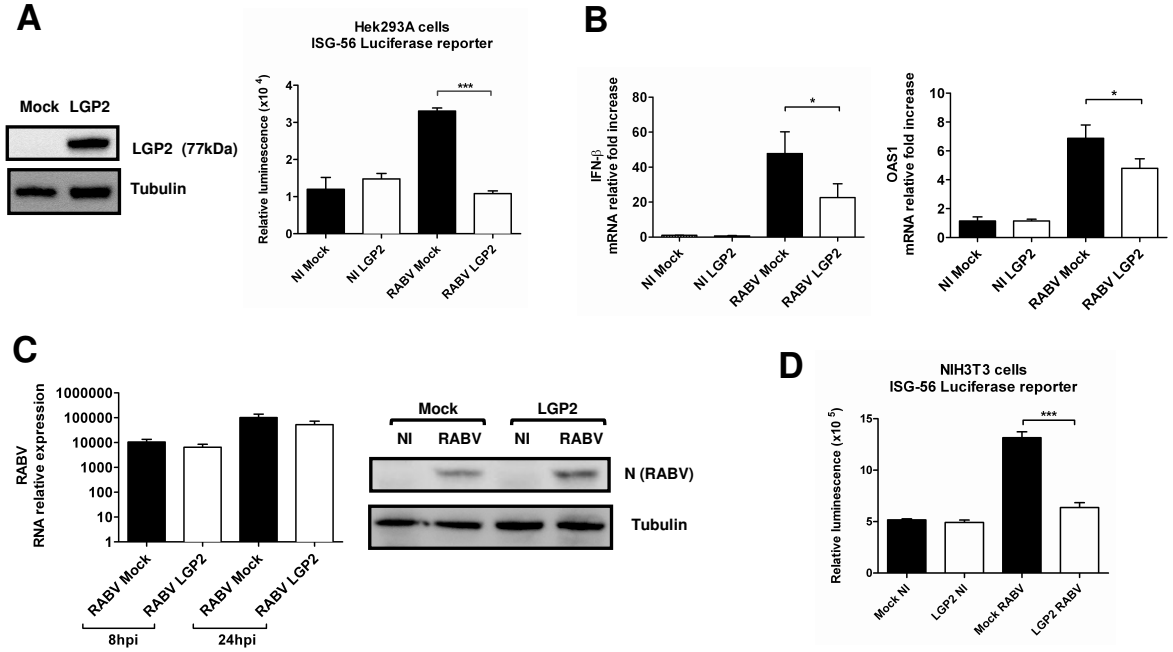
Figure 8. LGP2 inhibits RABV induced B7-H expression in both NS and dorsal root ganglia neurons. B7-H1 expression was measured by qRT-PCR (A) (n = 7–8) or by western blotting (B) in WT and LGP2 TG brain in the absence of infection (NI) or 8 and 11 days pi.

JVI Accepts published online ahead of print

Data are represented as mean ± SEM. (** $p \leq 0.005$, *** $p \leq 0.0005$). (C) Primary neurons from dorsal root ganglia of adult WT (upper row) and LGP2 TG (lower row) were infected with RABV. Neurons were immunostained with paired Abs directed against β III-tubulin (a marker for neurons), LGP2, RABV nucleocapsid, or B7-H1. The percentage of infected cells was similar (58.5% and 62.0% of RABV-infected cells) in WT and LGP2 TG cultures, respectively. Scale bar is 10 µm.

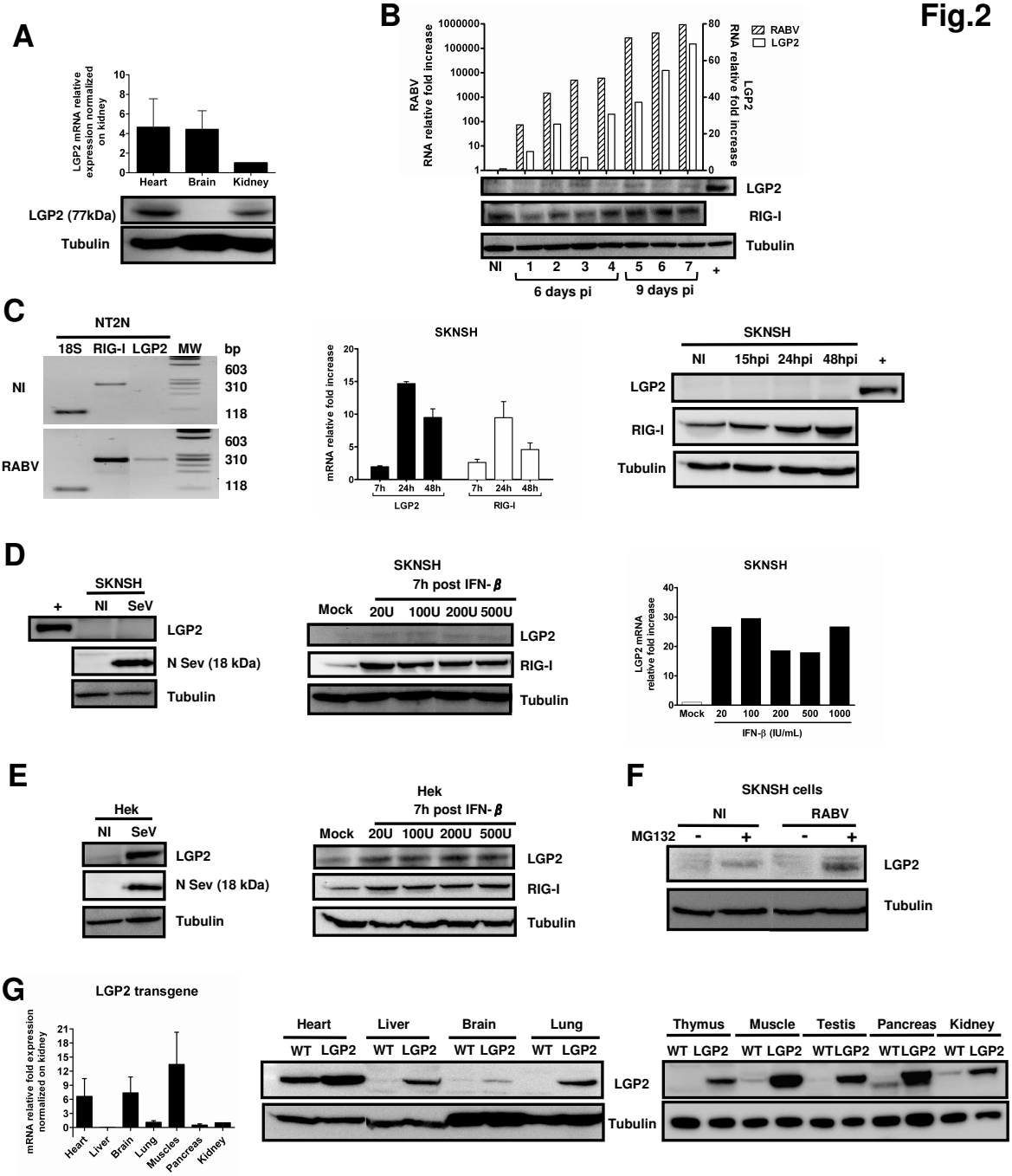
JVI Accepts published online ahead of print

Fig.1



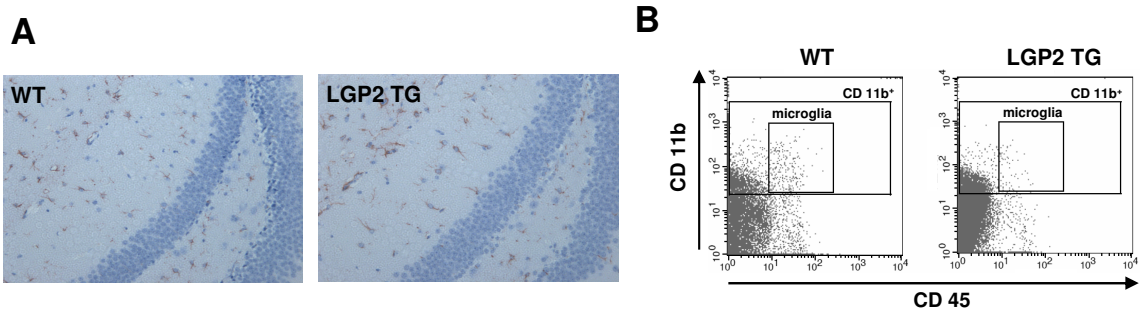
JVI Accepts published online ahead of print

Fig.2



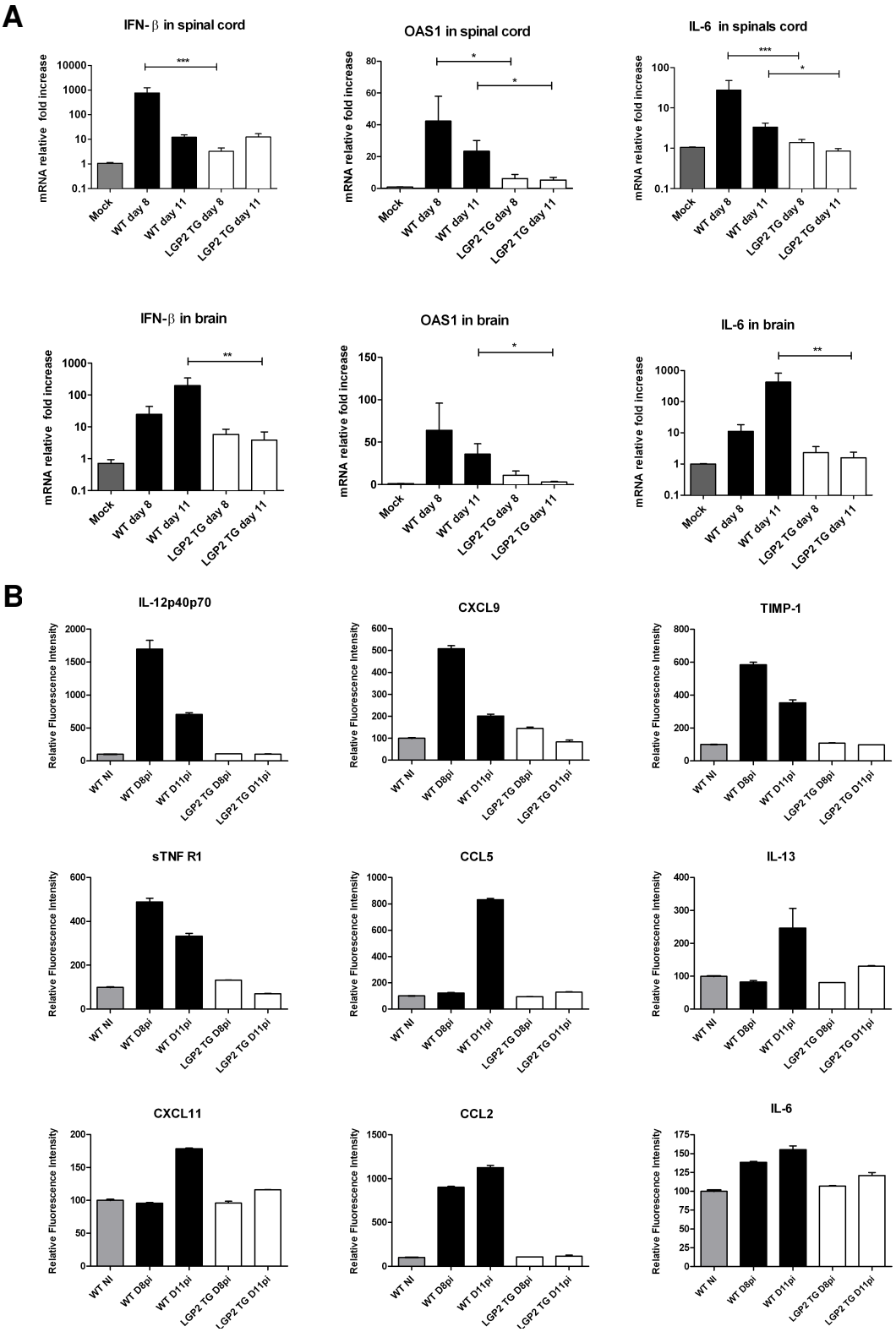
JVI Accepts published online ahead of print

Fig .3



JVI Accepts published online ahead of print

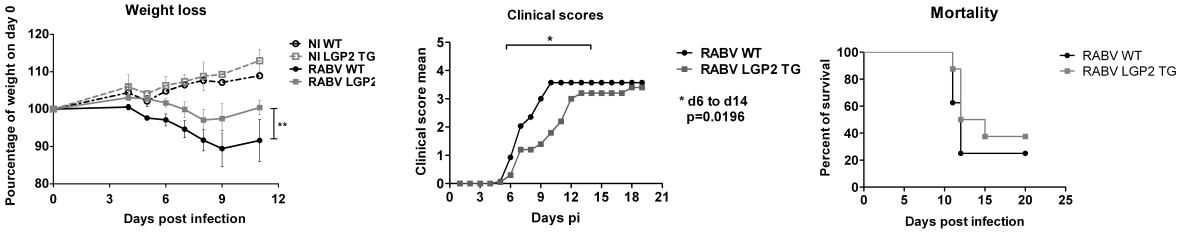
Fig.4



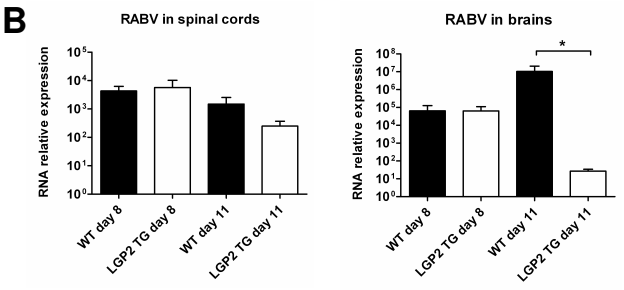
JVI Accepts published online ahead of print

Fig.5

A

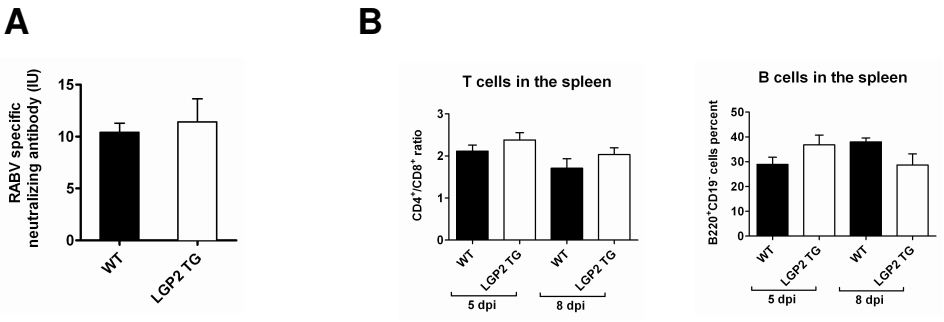


B



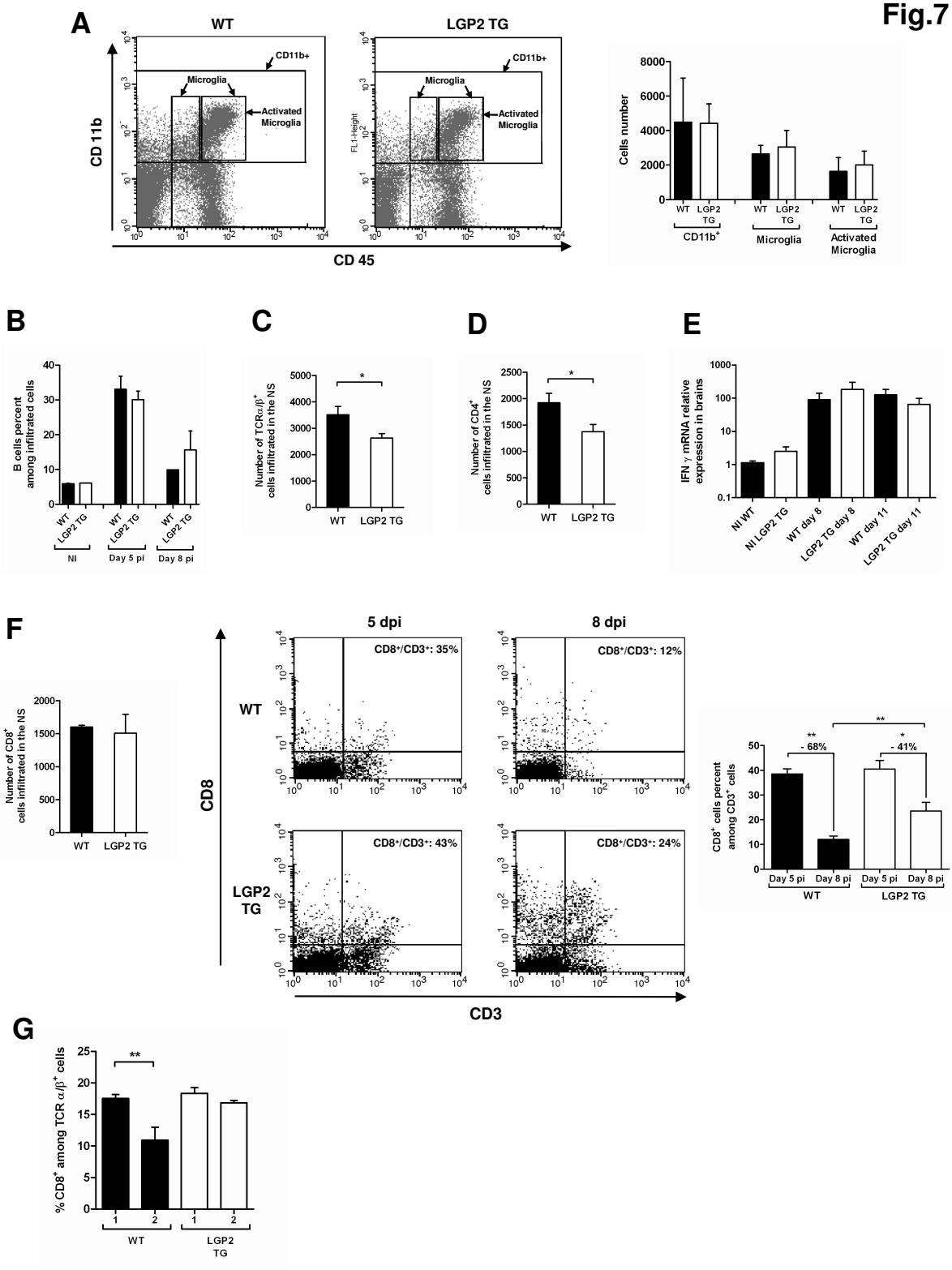
JVI Accepts published online ahead of print

Fig. 6



JVI Accepts published online ahead of print

Fig.7



JVI Accepts published online ahead of print

Fig.8

